

# Contents: Power and Delay

---

## **CMOS Static and Dynamic Power Consumption:**

**J Rabaey et al "Digital Integrated Circuits"**

## **Integration of III/V HEMTs on Si :**

**S Datta et al IEEE Electron Dev. Lett. 28, 2007 p 685 " Ultrahigh-Speed 0.5 V Supply ..."**

## **HEMTS for Beyond-CMOS:**

**D-H Kim et al IEEE Trans. Electron Dev. 54, 2007 p 2606 " Logic Suitability of 50 nm ..."**

# CMOS Dynamic and Static Power Consumption

---

Advantages with CMOS:

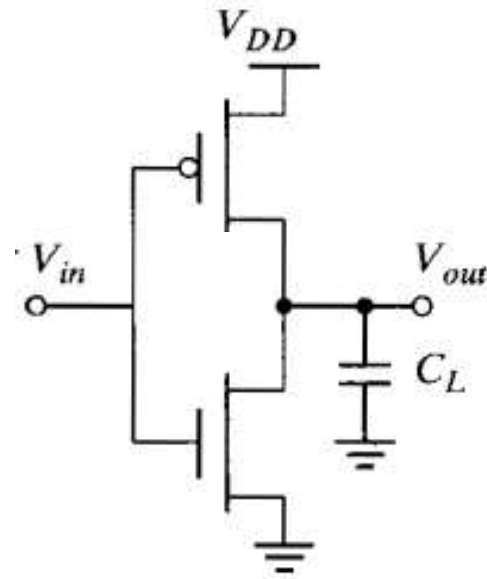
Full logic swing

High noise margin

Superior robustness

Low steady state power consumption

Robust low-power digital technology



$V_{out} = V_{in}$  for next stage

$C_L$  both parasitics and gate capacitance

# Dynamic Power Consumption

Advantages with CMOS:

Full logic swing

High noise margin

Superior robustness

Absence of steady state power consumption

**Calculate the charging energy during one switching event!**

Calculate the charging energy:

$$E_{VDD} = \int_0^{\infty} i_{VDD}(t) V_{DD} dt = V_{DD} \int_0^{\infty} C_L \frac{dv_{out}}{dt} dt = C_L V_{DD} \int_0^{V_{DD}} dv_{out} = C_L V_{DD}^2$$

Calculate the stored energy:

$$E_C = \int_0^{\infty} i_{VDD}(t) v_{out} dt = \int_0^{\infty} C_L \frac{dv_{out}}{dt} v_{out} dt = C_L \int_0^{V_{DD}} v_{out} dv_{out} = \frac{C_L V_{DD}^2}{2}$$

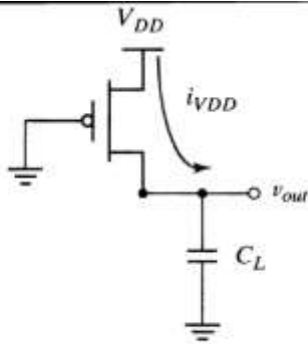
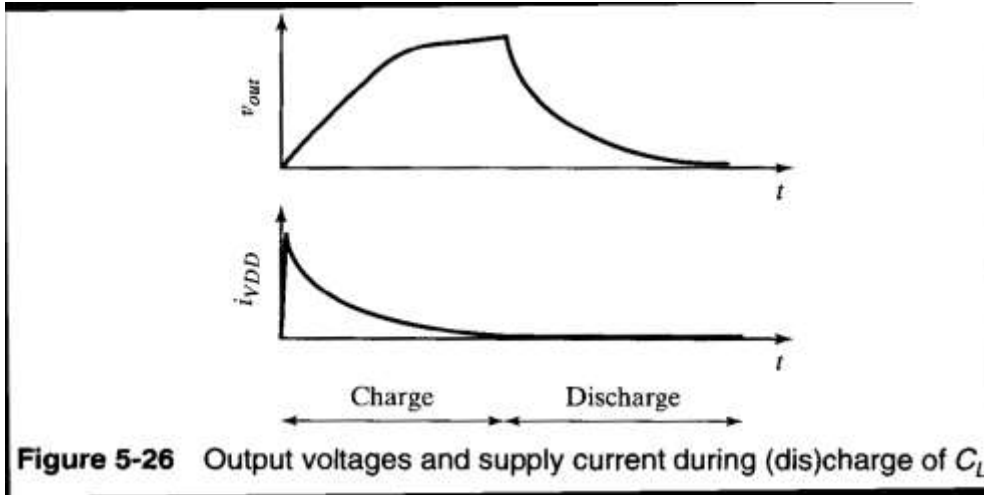


Figure 5-25 Equivalent circuit during the low-to-high transition.

# Dynamic Power Consumption



During charging (low-to-high transition) half energy is stored on capacitor, half energy is dissipated in the transistor

During discharging (high-to-low transition) half energy is stored on capacitor, the stored energy (half energy) is dissipated in the transistor

$$P_{dyn} = C_L V_{DD}^2 f_{0 \rightarrow 1}$$

Example: 50 nm CMOS

$f = 2$  GHz  $C_L = 3$  fF/gate

$V_{DD} = 1.0$  V

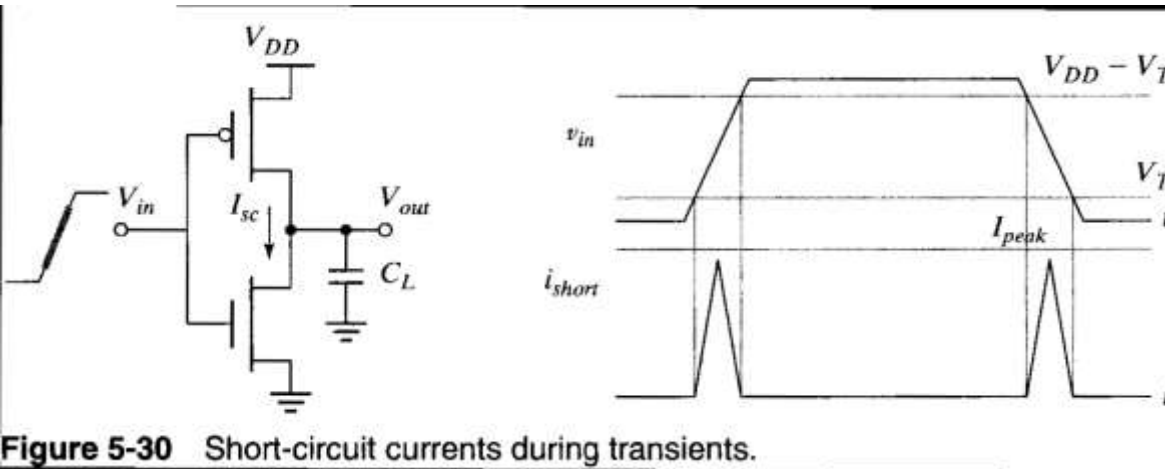
$P_{dyn} = 6$   $\mu$ W

Note: Not all transistors active!  
(effectively reduces frequency)

Voltage scaling reduces  $P_{dyn}$

Scaling reduces gate capacitance, but increases parasitic capacitance!

# Direct-Path Current Power Consumption



During the finite time switching, a direct current is flowing in the transistor pair

Assume triangular current peaks

$$E_{dp} = V_{DD} \frac{I_{peak} t_{sc}}{2} + V_{DD} \frac{I_{peak} t_{sc}}{2} = t_{sc} V_{DD} I_{peak}$$

$$P_{dp} = t_{sc} V_{DD} I_{peak} f = C_{sc} V_{DD}^2 f$$

This is typically a minor part of the power consumption

# Static Power Consumption: Drain Leakage

Leakage current typically 10-100 pA/ $\mu\text{m}^2$ . Drain area 50  $\text{nm}^2$  and 1 billion gates with  $V_{DD}=1.0$  V gives 0.5  $\mu\text{W}$ .

$$P_{stat} = I_{stat} V_{DD}$$

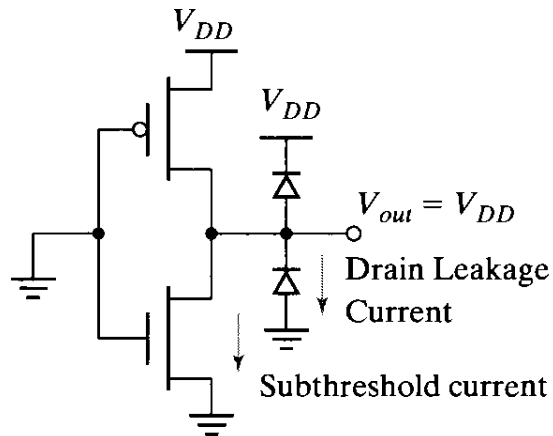


**Figure 5-34** Sources of leakage currents in CMOS inverter (for  $V_{in} = 0$  V).

Solution:

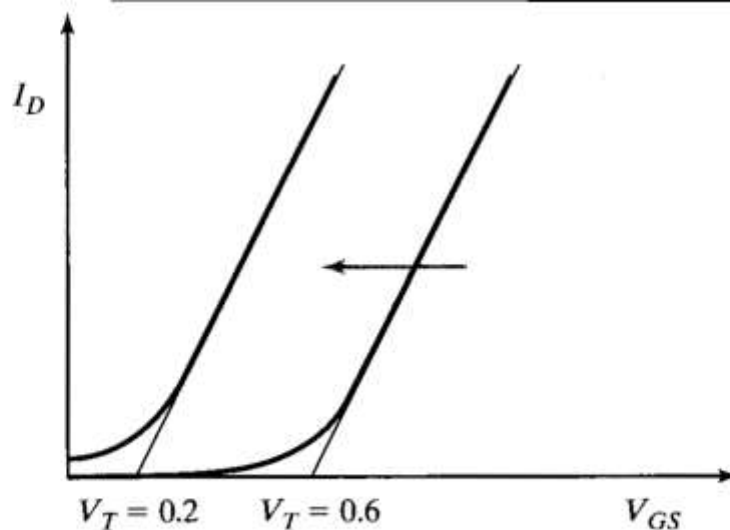
Use NWs to reduce channel leakage

Use SOI technology to reduce contact leakage

# Static Power Consumption: Subthreshold Leakage

As the drive voltage is reduced, the threshold voltage should also be scaled (recall  $V_t \sim V_{DD}/3$ ). This implies that the subthreshold current is substantially increased.

Consider a 50 nm NMOS transistor with SS of 60 mV/dec. and  $V_t=0.4$  V. At  $V_{GS}=0$  V it consumes about  $10^{-12}$  A. Reducing the threshold to 0.2 V increased the current a factor 300! In a 1 billion transistor operating at 1 V, we get a power consumption of  $10^9 \times 300 \times 10^{-12} \times 1.0 = 300$  mW!



Threshold voltage key parameter to balance on- and off-state

**Fundamental transistor problem!**

**Figure 5-35** Decreasing the threshold increases the subthreshold current at  $V_{GS} = 0$ .

# Put It All Together!

Dynamic during switching

Direct during switching

Total leakage current

$$P_{tot} = P_{dyn} + P_{dp} + P_{stat} = \left( \underbrace{C_L V_{DD}^2}_{\text{Typically dominant}} + \underbrace{V_{DD} I_{peak} t_s}_{\text{Can be reduced}} \right) f_{0 \rightarrow 1} + \underbrace{V_{DD} I_{leak}}_{\text{Will be more important in scaled technologies}}$$

Typically dominant

Can be reduced

Will be more important in scaled technologies



# The Power-Delay Product

---

Introduce the power-delay product as a quality measure of a logic gate:

$$PDP = P_{av} t_p$$

If the gate is switched at full speed, the PDP corresponds to the average energy consumed per switching event (0->1 or 1->0 transition)

$$PDP = C_L V_{DD}^2 f_{\max} t_p = \frac{C_L V_{DD}^2}{2}$$

# Better, The Energy-Delay Product

---

Introduce the energy-delay product, which balances the performance and energy consumption!

$$EDP = PDP \times t_p = P_{av} t_p^2 = \frac{C_L V_{DD}^2}{2} t_p$$

$t_p$  is the propagation delay (gate delay) and  $f_{\max} = 1/(2t_p)$

# Voltage Dependence on EDP!!!

$$EDP = PDP \times t_p = P_{av} t_p^2 = \frac{C_L V_{DD}^2}{2} t_p$$

$$t_p \approx \frac{\alpha C_L V_{DD}}{(V_{DD} - V_T)^2}$$

$$EDP = \frac{\alpha C_L^2 V_{DD}^3}{2(V_{DD} - V_T)^2}$$

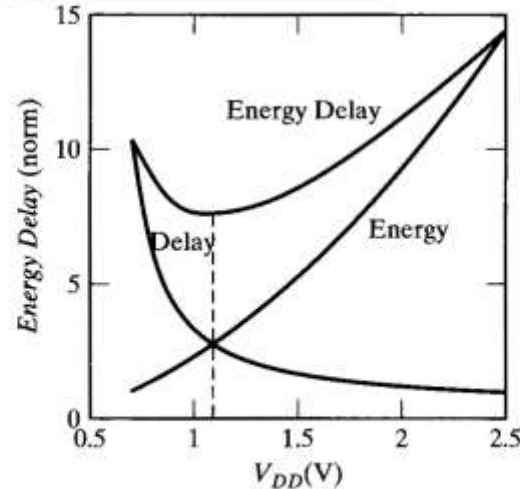


Figure 5-36 Normalized delay, energy, and energy-delay plots for CMOS inverter in 0.25- $\mu\text{m}$  CMOS technology.

Increase  $V_d$ :

Speed improves  
(higher current)  
Energy increases  
(more charge)  
Optimum!

Extra (model validation):

$$t_p = \frac{t_{pHL} + t_{pLH}}{2} = \ln 2 \times C_L \left( \frac{R_{eqn} + R_{eqp}}{2} \right)$$

$$t_{pHL} = \ln 2 \times \frac{3}{4} \frac{C_L V_{DD}}{(W/L)_n \left( \mu_n \varepsilon_{ox} / t_{ox} \right) (V_{DD} - V_{Tp})^2}$$

RC-time constant during switching

Use transistor equations to derive the effective transistor resistance

Nanoelectronics: Power and Delay

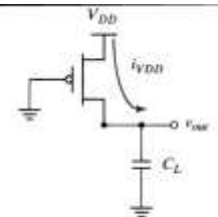


Figure 5-25 Equivalent circuit during the low-to-high transition.

# Ultrahigh-Speed 0.5 V Supply Voltage $\text{In}_{0.7}\text{Ga}_{0.3}\text{As}$ Quantum-Well Transistors on Silicon Substrate

Suman Datta, *Senior Member, IEEE*, G. Dewey, J. M. Fastenau, *Member, IEEE*, M. K. Hudait, D. Loubychev, W. K. Liu, *Senior Member, IEEE*, M. Radosavljevic, W. Rachmady, and R. Chau, *Fellow, IEEE*

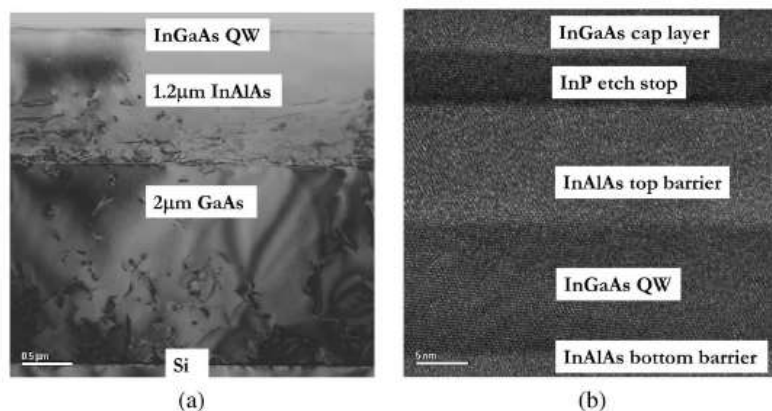


Fig. 1. Cross-sectional TEM images of  $\text{In}_{0.7}\text{Ga}_{0.3}\text{As}$  QW structures on Si using metamorphic buffer architecture: (a) Entire layer structure. (b) magnification of  $\text{In}_{0.7}\text{Ga}_{0.3}\text{As}$  QW along with bottom and top barrier layers. The misfit dislocations are predominantly contained in the buffer layer.

- buffer layer techniques are available
- comparable mobility

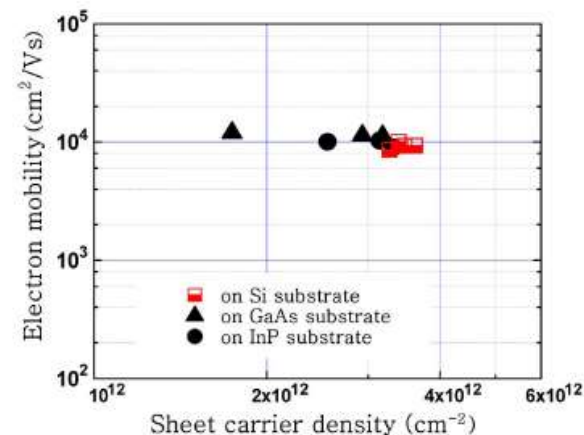


Fig. 2. Electron mobility versus sheet carrier density in n-channel  $\text{In}_{0.7}\text{Ga}_{0.3}\text{As}$  QW device layers grown on Si, GaAs, and InP substrates. In all cases,  $\text{In}_{0.52}\text{Al}_{0.48}\text{As}$  is the bottom and top barrier layer.

# Comparable RF-data!

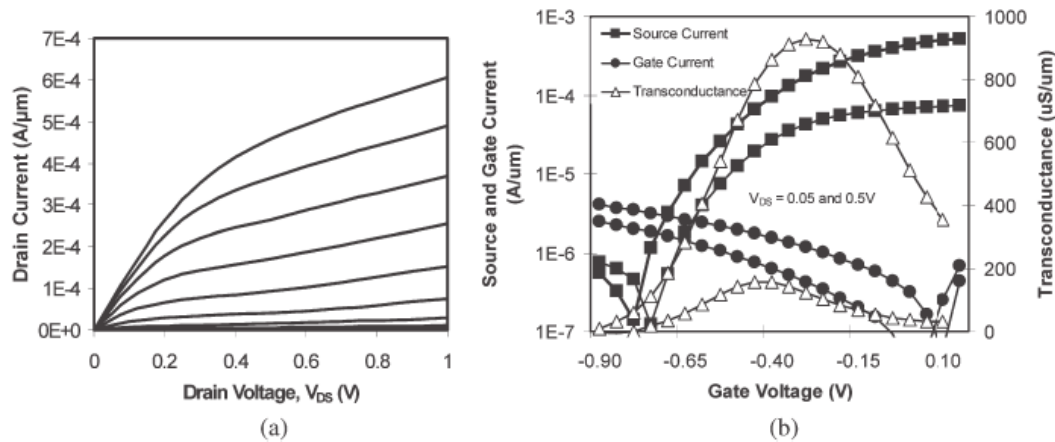


Fig. 3. (a) Output characteristic for 80-nm  $L_g$   $\text{In}_{0.7}\text{Ga}_{0.3}\text{As}$  QW transistor on 3.2- $\mu\text{m}$  metamorphic buffer on silicon (gate voltage  $V_G$  is swept from 0.0 to  $-0.8$  V in  $-0.1$ -V steps). (b) Transfer characteristic for 80-nm  $L_g$   $\text{In}_{0.7}\text{Ga}_{0.3}\text{As}$  QW transistor on 3.2- $\mu\text{m}$  buffer on silicon with  $V_{DS} = 0.5$  and  $0.05$  V. Peak transconductance  $g_m$  for this device was  $930 \mu\text{S}/\mu\text{m}$  at  $V_{DS} = 0.5$  V.

- well behaved IV characteristics!
- good DC numbers at 80 nm  $L_g$
- comparable RF data to lattice matched devices

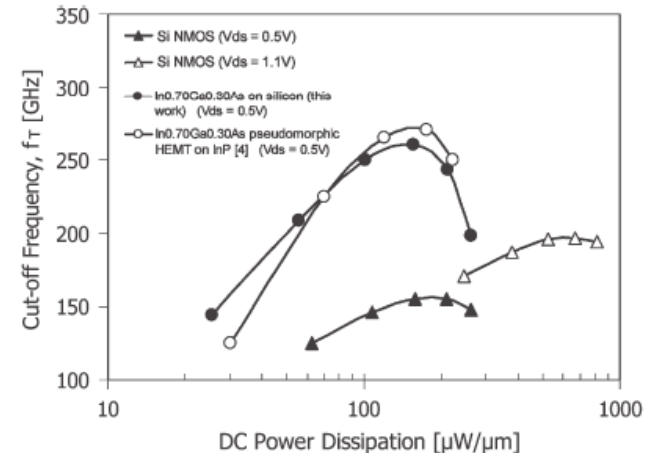


Fig. 4. Plot of deembedded unity gain cutoff frequency as a function of dc power dissipation for 0.5-V  $V_{DS}$  80-nm  $L_g$   $\text{In}_{0.7}\text{Ga}_{0.3}\text{As}$  QW transistors on both silicon and InP substrates, benchmarked against 60-nm  $L_g$  silicon NMOS transistors at  $V_{DS} = 0.5$  and  $1.1$  V.

# Logic Suitability of 50-nm $\text{In}_{0.7}\text{Ga}_{0.3}\text{As}$ HEMTs for Beyond-CMOS Applications

Dae-Hyun Kim, Jesús A. del Alamo, Jae-Hak Lee, and Kwang-Seok Seo

n+ Cap	InGaAs, $x = 0.53$	20 nm
Stopper	InP	6 nm
Barrier	InAlAs, $x = 0.52$	8 nm
$\delta$ -doping	Si	-
Spacer	InAlAs, $x = 0.52$	3 nm
Channel	InGaAs, $x = 0.53$	3 nm
	InGaAs, $x = 0.7$	8 nm
	InGaAs, $x = 0.53$	4 nm
Buffer	InAlAs, $x = 0.52$	500 nm

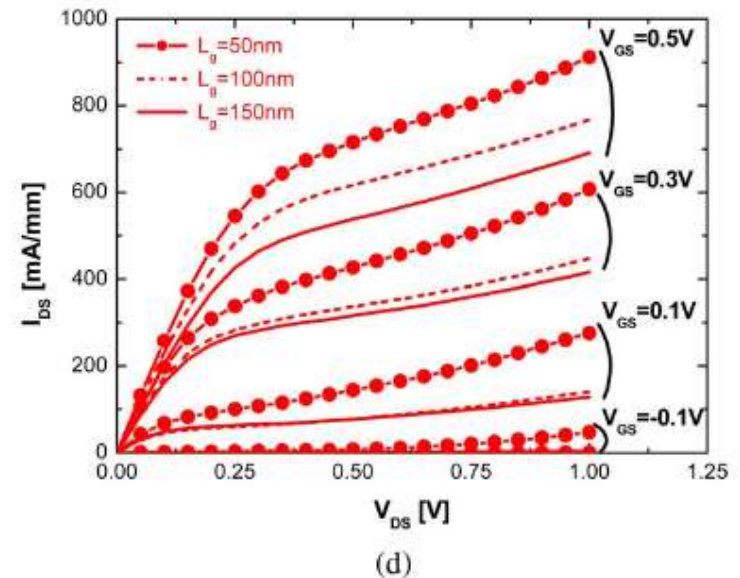
3 Inch S. I. InP Substrate

TABLE I  
DETAILED GATE STRUCTURAL INFORMATION FOR FOUR TYPES OF  $\text{In}_{0.7}\text{Ga}_{0.3}\text{As}$  HEMTs THAT ARE FABRICATED IN THIS PAPER

	Type-A	Type-B	Type-C	Type-D
Barrier	InP/ $\text{In}_{0.52}\text{Al}_{0.48}\text{As}$	$\text{In}_{0.52}\text{Al}_{0.48}\text{As}$	$\text{In}_{0.52}\text{Al}_{0.48}\text{As}$	$\text{In}_{0.52}\text{Al}_{0.48}\text{As}$
Stack	Ti/Pt/Au	Ti/Pt/Au	Pt/Ti/Mo/Au	Buried-Pt/Ti/Mo/Au
$t_{\text{ins}}$ [nm]	17	11	11	7
$\Phi_{\text{B}}$ [eV]	$\sim 0.4$	$\sim 0.6$	$\sim 0.7$	$\sim 0.8$

Fig. 1. Epitaxial layer structure of the  $\text{In}_{0.7}\text{Ga}_{0.3}\text{As}$  HEMTs that are fabricated in this paper.

- 4 types of transistors
- Schottky barrier and insulator thickness
- good DC characteristics
- weak scaling with gate length



Nanoelectronics: Power and Delay

# Scaling with Schottky barrier and insulator thickness

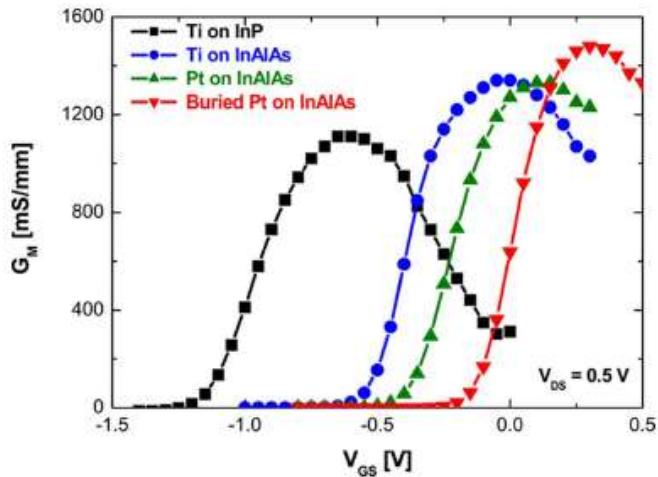


Fig. 5. Transconductance ( $G_m$ ) characteristics of all 50-nm  $\text{In}_{0.7}\text{Ga}_{0.3}\text{As}$  HEMTs at  $V_{DS} = 0.5$  V.

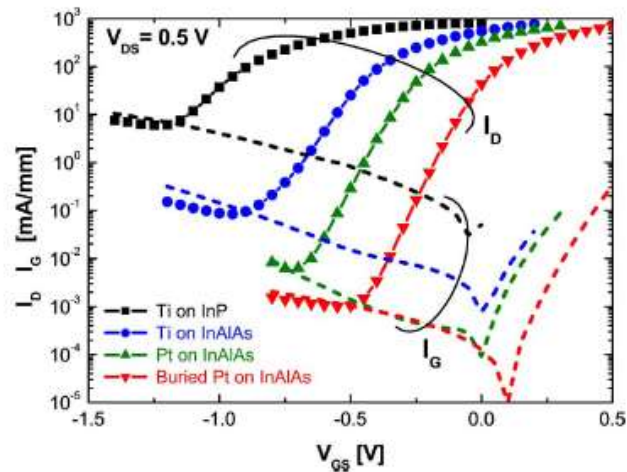


Fig. 6. Semilog plot of  $I_D$  and  $I_G$  of all 50-nm  $\text{In}_{0.7}\text{Ga}_{0.3}\text{As}$  HEMTs at  $V_{DS} = 0.5$  V.

- Tight control needed to improve the performance

TABLE II  
SUMMARY OF LOGIC FIGURES OF MERIT FOR FOUR TYPES  
OF 50-nm  $\text{In}_{0.7}\text{Ga}_{0.3}\text{As}$  HEMTs

	$V_T$ [V]	DIBL [mV/V]	S [mV/dec]	$I_{ON}/I_{OFF}$
Type-A	-1.10	300	200	63
Type-B	-0.65	220	130	$1 \times 10^3$
Type-C	-0.55	180	100	$7.2 \times 10^3$
Type-D	-0.20	160	86	$1.7 \times 10^4$

# Improved speed and/or reduced power consumption

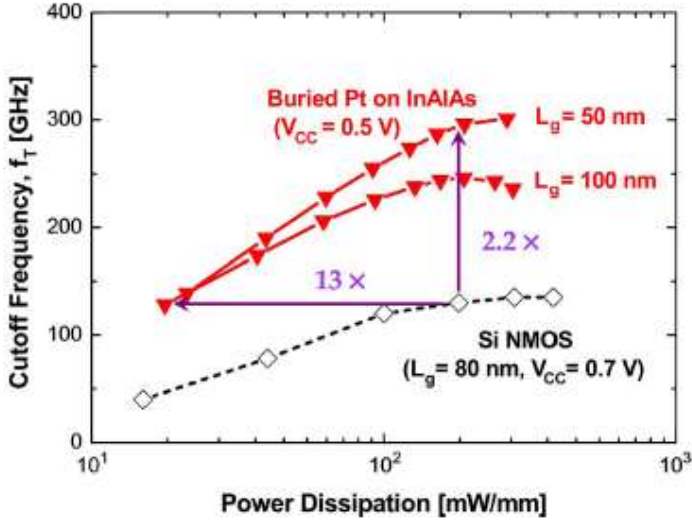


Fig. 11. Cutoff frequency ( $f_T$ ) of our 50- and 100-nm type D  $\text{In}_{0.7}\text{Ga}_{0.3}\text{As}$  HEMTs and 80-nm Si MOSFETs as a function of the dc power dissipation.

- Depending on bias condition benefits can be found in the areas of speed and/or power dissipation

- Well selected technology is required to maximize  $I_{ON}/I_{OFF}$  ratio

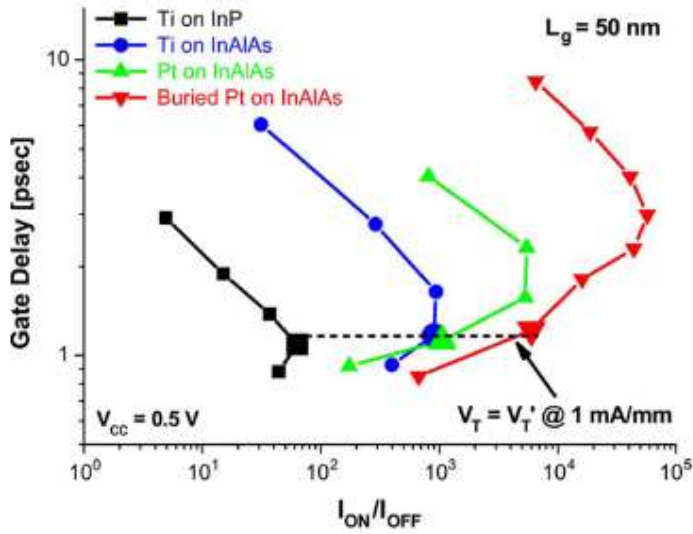


Fig. 14. Gate delay ( $CV/I$ ) of all 50-nm  $\text{In}_{0.7}\text{Ga}_{0.3}\text{As}$  as a function of  $I_{ON}/I_{OFF}$ .



# 22FFL: A High Performance and Ultra Low Power FinFET Technology for Mobile and RF Applications

B. Sell, B. Bigwood, S. Cha, Z. Chen, P. Dhage, P. Fan, M. Giraud-Carrier, A. Kar, E. Karl, C.-J. Ku, R. Kumar, T. Lajoie, H.-J. Lee, G. Liu, S. Liu, Y. Ma, S. Mudanai, L. Nguyen, L. Paulson, K. Phoa, K. Pierce, A. Roy, R. Russell, J. Sandford, J. Stoeger, N. Stojanovic, A. Sultana, J. Waldemer, J. Wan, W. Xu, D. Young\*, J. Zhang, Y. Zhang and P. Bai

Logic Technology Development, \*Corporate Quality Network, Intel Corporation, Hillsboro, OR, USA  
email: [bernhard.sell@intel.com](mailto:bernhard.sell@intel.com)

Device	High Performance Logic Transistor			Low Power Logic Transistor			Ultra Low Power Logic Transistor	Analog Transistor			High Voltage Transistor				
	ULVT	LVT	LPLVT	HP	Nom	LP	LL	AL	AL	AL	TGLV	TGMV	TGHV		
VDD [Volt]	0.7	0.7	0.7	0.7	0.7	0.7	0.7	0.7	0.7	0.7	1.2	1.5	1.8		
Gate Pitch [nm]	108	108	108	108	108	108	144	144	216	270	216	216	270		
Fin Pitch [nm]	45	45	45	45	45	45	45	45	45	45	45	45	45		
Tox	Thin	Thin	Thin	Thin	Thin	Thin	Thick	Thin	Thin	Thin	Thick	Thick	Thick		
Performance Metric	NMOS/PMOS						GM*Rout			NMOS/PMOS					
	Idsat/Ioff [mA/um]									Idsat [mA/um]					
Value	1.24/1.22 @ 0.7V, 10nA/um			0.81/0.81 @ 0.7V, 100pA/um			0.10/0.10 @ 0.7V, 1pA/um			47	54	60	0.77/ 0.61	1.01/ 0.87	1.11/ 1.02

Table 1. Transistor design rules and electrical characteristics for logic, analog and high voltage transistors developed for 22FFL.

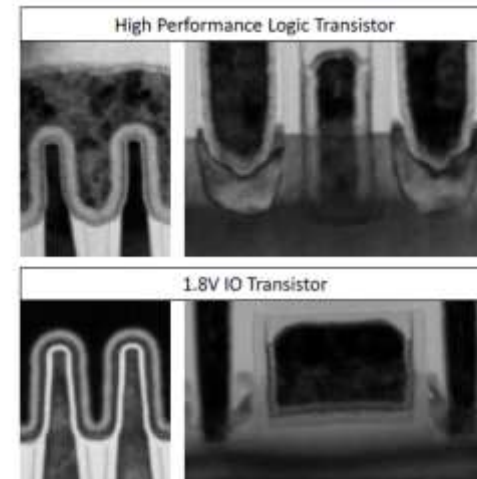


Fig. 1. Fin and gate cut TEMs of logic and 1.8V IO transistors.

# 22FFL: A High Performance and Ultra Low Power FinFET Technology for Mobile and RF Applications

B. Sell, B. Bigwood, S. Cha, Z. Chen, P. Dhage, P. Fan, M. Giraud-Carrier, A. Kar, E. Karl, C.-J. Ku, R. Kumar, T. Lajoie, H.-J. Lee, G. Liu, S. Liu, Y. Ma, S. Mudanai, L. Nguyen, L. Paulson, K. Phoa, K. Pierce, A. Roy, R. Russell, J. Sandford, J. Stoeger, N. Stojanovic, A. Sultana, J. Waldemer, J. Wan, W. Xu, D. Young\*, J. Zhang, Y. Zhang and P. Bai

Logic Technology Development, \*Corporate Quality Network, Intel Corporation, Hillsboro, OR, USA  
 email: [bernhard.sell@intel.com](mailto:bernhard.sell@intel.com)

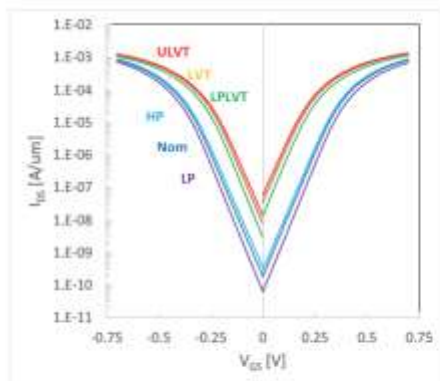


Fig. 5.  $I_{DS}-V_{GS}$  curves demonstrating low subthreshold slope and DIBL for all logic devices.

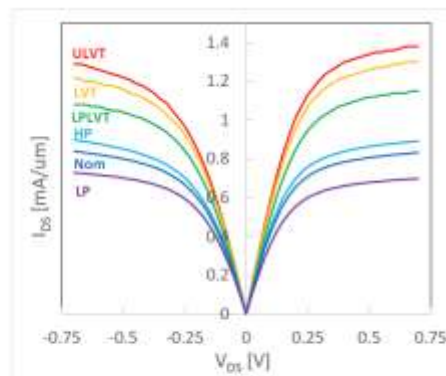


Fig. 6. Balanced  $I_{DS}-V_{DS}$  characteristics for all logic transistors.

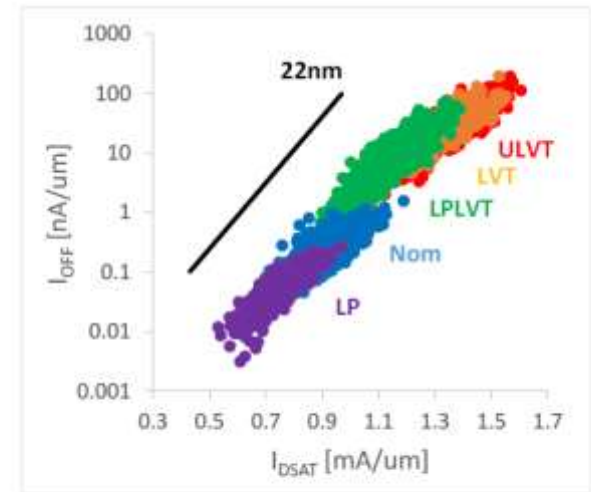


Fig. 3. NMOS  $I_{DSat}$  vs.  $I_{off}$  showing 57% gain over 22nm HP transistors presented in [1].

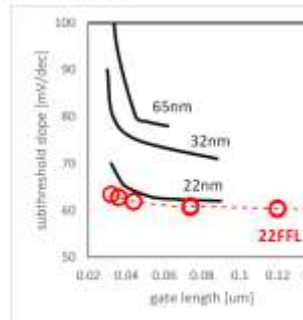


Fig. 7. Channel length dependence of the subthreshold slope compared to previous technologies.

# Improved speed and/or reduced power consumption

## Intel 22nm FinFET (22FFL) Process Technology for RF and mmWave Applications and Circuit Design Optimization for FinFET Technology

H.-J. Lee, S. Rami, S. Ravikumar, V. Neeli, K. Phoa, B. Sell, and Y. Zhang  
Logic Technology Development, Intel Corporation, Hillsboro, Oregon, USA, email: hyung-jin.lee@intel.com

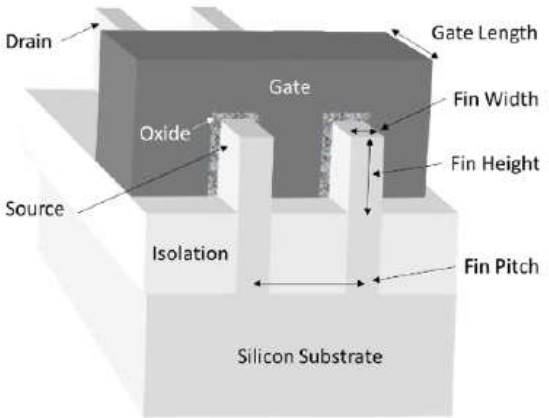


Figure 1: 3D view of FinFET device structure

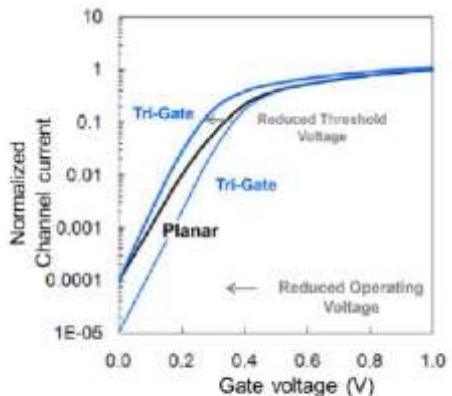
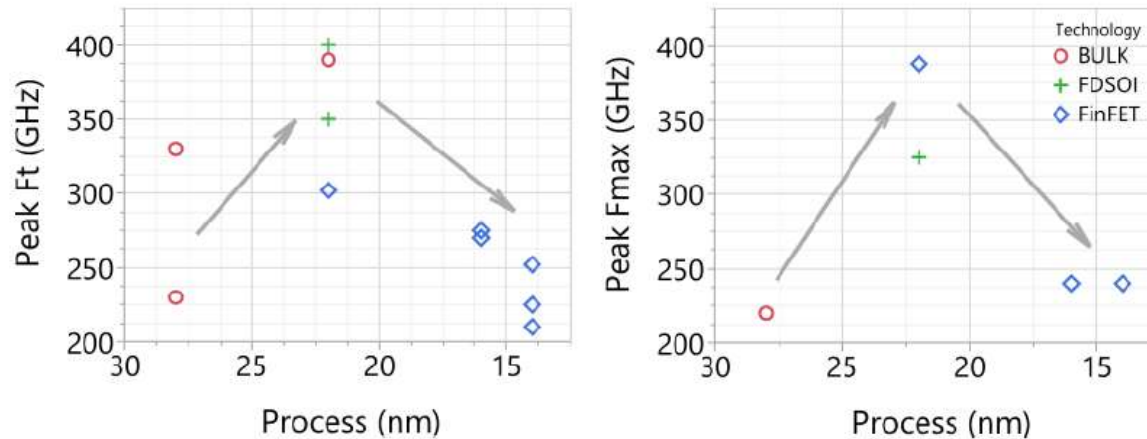


Figure 2: I-V curves of FinFET and Planar demonstrating DIBL improvement by FinFET technologies

- Tri-gates optimized for RF-operation

# Parasitics are Limiting Performance at Scaled Nodes



- Currently best performance is obtained at about 20 nm node!

Figure 5:  $f_t$  and  $f_{max}$  trends by process node: both  $f_t$  and  $f_{max}$  reach the peak performance around 20 ~ 25nm due to the excessive parasitic capacitance by high density interconnect

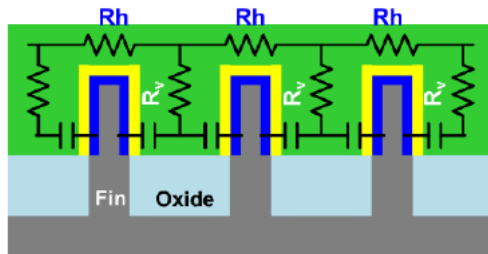


Figure 3: FinFET gate resistance structure: Horizontal resistance ( $R_h$ ) and Vertical resistance ( $R_v$ ) surrounding fin structures

- Parasitics are related to gate resistance and capacitances (lack of space)